Lab Course: Bell's Inequality and Quantum Tomography

Revision Nov. 2014

Contents

1 Qubits and entanglement **2**

1.1 Characterization of qubit states 2

1.1.1 What is a qubit? 2

1.1.2 Two-qubits states 4

1.1.3 Bell States and entanglement 6

1.2 EPR paradox and Bell's inequality 6

1.2.1 EPR paradox 6

1.2.2 Bell's - CHSH inequality 8

1.3 Density operator 11

1.3.1 Mixed states 11

1.3.2 Derivations of the density operator 12

2 Experimental setup **16**

2.1 Generation of the entangled photons 16

2.2 Polarization analysis and the detection system 19

2.3 Software for the measurements 23

3 Experimentation **25**

Bell's Inequality & Quantum Tomography

Advanced Laboratory Course

Entanglement lies at the heart of quantum information processing and leads to many interesting fields of research. On the one hand it is the key element for application-oriented quantum physics like quantum cryptography, teleportation or quantum computation and on the other hand its characteristics can be used for a fundamental test of non-classical properties of quantum theory. During this lab course the distinctive features of two-photon entanglement, like the violation of a Bell inequality, shall be explained and also the entangled state will be reconstructed completely through quantum tomography.

1 Qubits and entanglement

First of all, the theoretical framework of two-photon entangled states is described. Therefore, the basic properties of quantum mechanics are summarized briefly (for further details see [6]) and afterwards are adapted to two-photon entanglement.

1.1 Characterization of qubit states

1.1.1 What is a qubit?

In general, a classical physical state is described by a minimal set of physical quantities which provides full information about the considered physical system. In classical mechanics the state of a physical system is completely described by the generalized coordinate $\vec{q}$ and the generalized momentum $\vec{p}$. By contrast in quantum mechanics a physical state is given by a vector in an, in general, infinite-dimensional complex vector space - the Hilbert space [17]. In our case the dimension of the Hilbert space for a single particle is reduced to two dimensions, because we use the polarization degree of freedom of photons. In 1995 Schumacher established the word "Qubit" for such a state as the quantum mechanical analogue of the classical bit. Generally, a qubit is a two-level quantum state defined as a vector of a Hilbert space. Due to the quantum superposition principle any normalized linear combination of two states is a possible state again. Here the two orthogonal states can be encoded in the horizontal $|H\rangle$ and vertical $|V\rangle$ polarization. So a general qubit state can be written as the superposition of the two basic vectors:

$$|\psi\rangle = a\,|H\rangle + b\,|V\rangle \mathrel{\widehat{=}} \begin{pmatrix} a \\ b \end{pmatrix} \text{ with } |a|^2 + |b|^2 = 1 \tag{1.1}$$

By ignoring a global phase and considering the normalization implicitly [23], this can be expressed as

$$|\psi_{\theta,\phi}\rangle = \cos\left(\frac{\theta}{2}\right)|H\rangle + e^{(i\phi)}\sin\left(\frac{\theta}{2}\right)|V\rangle \text{ with } \theta \in [0,\pi]\,,\ \phi \in [0,2\pi] \tag{1.2}$$

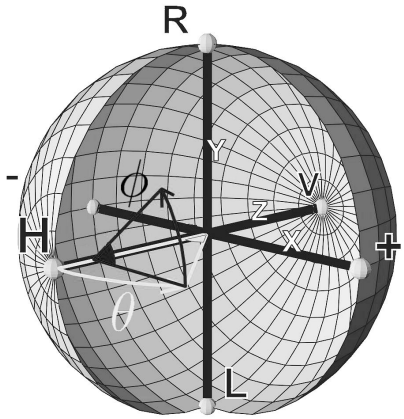

Figure 1.1: Bloch sphere represents the Hilbert space of one qubit. On the three orthogonal axis (X,Y,Z) the eigenvectors of the Pauli matrices ($\widehat{\sigma}_x, \widehat{\sigma}_y, \widehat{\sigma}_z$) are situated (from [10]).

The full Hilbert space of a single qubit can be illustrated by the Bloch sphere, as seen in figure 1.1. A pure state $|\psi\rangle$ is represented by a vector ending at the surface of the Bloch sphere, while a mixed state lies within the sphere. $|\psi\rangle$ is reached by rotating $|H\rangle$ by an angle θ around the Y axis and by ϕ around the Z axis.

In quantum mechanics a measurement is represented by observables, i.e. hermitian operators [6]. More precisely, it is defined as the projection onto one of the eigenstates of the observable and the measurement result is the corresponding eigenvalue. It is convenient to choose the Pauli spin matrices $\widehat{\sigma}_x, \widehat{\sigma}_y, \widehat{\sigma}_z$ and the identity 1 as the operators acting on the 2-dimensional Hilbert space, because their eigenvectors form an orthogonal basis on the 2-D Hilbert space [10]. In figure 1.1 the basis of the Bloch sphere is given by the eigenvectors of the Pauli spin matrices.

$$\begin{aligned}
\widehat{\sigma}_x &= \begin{pmatrix} 0 & 1 \\ 1 & 0 \end{pmatrix} = |H\rangle\langle V| + |V\rangle\langle H| \\
\widehat{\sigma}_y &= \begin{pmatrix} 0 & -i \\ i & 0 \end{pmatrix} = i(|V\rangle\langle H| - |H\rangle\langle V|) \\
\widehat{\sigma}_z &= \begin{pmatrix} 1 & 0 \\ 0 & -1 \end{pmatrix} = |H\rangle\langle H| - |V\rangle\langle V|
\end{aligned} \tag{1.3}$$

A measurement of a qubit can be associated to two possible eigenvalues +1 or -1 and the corresponding eigenvectors are defined as follows:

$$\begin{aligned}
\widehat{\sigma}_x\,[\frac{1}{\sqrt{2}}(|H\rangle \pm |V\rangle)] &= \widehat{\sigma}_x\ |+/-\rangle \ = \pm\ |+/-\rangle \\
\widehat{\sigma}_y\,[\frac{1}{\sqrt{2}}(|H\rangle \pm i\,|V\rangle)] &= \widehat{\sigma}_y\ |R/L\rangle \ = \pm\ |R/L\rangle \\
\widehat{\sigma}_z\ |H/V\rangle \ &= \pm |H/V\rangle
\end{aligned} \tag{1.4}$$

So $|+/-\rangle$ corresponds to $\pm 45°$ linear and $|R/L\rangle$ to right/ left circular polarized photons.

A general observable $\widehat{\sigma}_{\theta,\phi}$ can be defined in terms of the Pauli operators as:

$$\widehat{\sigma}_{\theta,\phi} = \cos(\phi)\sin(\theta)\,\widehat{\sigma}_x + \sin(\phi)\sin(\theta)\,\widehat{\sigma}_y + \cos(\theta)\,\widehat{\sigma}_z \tag{1.5}$$

For example:

$$\widehat{\sigma}_{0,0} = \widehat{\sigma}_z \quad \widehat{\sigma}_{\frac{\pi}{2},0} = \widehat{\sigma}_x \quad \widehat{\sigma}_{\frac{\pi}{2},\frac{\pi}{2}} = \widehat{\sigma}_y \tag{1.6}$$

Let us now consider, that we want to measure only the $|H\rangle$ basis vector of the state $|\psi_{\theta,\phi}\rangle$. Therefore, we can calculate the probability of occurrence with the expectation value of the projector P_H which is defined as follows:

$$P_H = |H\rangle\langle H| = \frac{1}{2}(1+\widehat{\sigma}_z), \tag{1.7}$$

$$\langle\psi_{\theta,\phi}|P_H|\psi_{\theta,\phi}\rangle = \cos^2\left(\frac{\theta}{2}\right). \tag{1.8}$$

And consequently a projector $P^{\pm}_{\theta,\phi}$ is given by:

$$P^{\pm}_{\theta,\phi} = |\psi_{\theta,\phi}\rangle\langle\psi_{\theta,\phi}| = \frac{1}{2}(1+\widehat{\sigma}_{\theta,\phi}). \tag{1.9}$$

In the last step the single qubit correlation for the pure states $|\psi\rangle$ can be calculated in a general basis setting $\widehat{\sigma}_{\theta,\phi}$ according to:

$$E(\theta,\phi) = \langle\psi|\widehat{\sigma}_{\theta,\phi}|\psi\rangle = \langle\psi|P^{+}_{\theta,\phi} - P^{-}_{\theta,\phi}|\psi\rangle = p^{+}_{\theta,\phi} - p^{-}_{\theta,\phi} \tag{1.10}$$

with the probabilities of occurrence $p^{+}_{\theta,\phi}$, $p^{-}_{\theta,\phi}$ [25].

1.1.2 Two-qubits states

In this experiment the spatial separation of the two qubits as another degree of freedom allows us to distinguish them, i.e. the two qubits can be numbered. In this section we want to describe this state theoretically: Assuming that the two qubits represent a single system, the corresponding Hilbert space $\mathcal{H}$ is given by the tensor product of the two preceding Hilbert spaces $\mathcal{H}_1$ and $\mathcal{H}_2$ spanning the vector space of each qubit [6], i.e.

$$\mathcal{H} = \mathcal{H}_1 \otimes \mathcal{H}_2. \tag{1.11}$$

A basis of $\mathcal{H}$ can be obtained by defining the tensor product of the single qubit basis vectors:

$$\begin{aligned} |HH\rangle &= |H\rangle\otimes|H\rangle \quad |HV\rangle = |H\rangle\otimes|V\rangle \\ |VH\rangle &= |V\rangle\otimes|H\rangle \quad |VV\rangle = |V\rangle\otimes|V\rangle \end{aligned} \tag{1.12}$$

So the most general two-qubit state in this basis is given by [25]:

$$|\Psi(a_{HH},a_{HV},a_{VH},a_{VV})\rangle = a_{HH}\,|HH\rangle + a_{HV}\,|HV\rangle + a_{VH}\,|VH\rangle + a_{VV}\,|VV\rangle \tag{1.13}$$

with $a_{HH},a_{HV},a_{VH},a_{VV} \in \mathbb{C}$ and $|a_{HH}|^2 + |a_{HV}|^2 + |a_{VH}|^2 + |a_{VV})|^2 = 1$.

States that can be expressed as a tensor product of single qubits are called separable or product states and any superposition of these is also an element of the Hilbert space $\mathcal{H}$. But superposition states cannot be written as a tensor product of the single qubits in general and therefore, these kind of states is called non-separable or entangled.
In order to characterize two-photon states, observables acting on the two qubit vector space have to be described. Let $\widehat{A}_1$ and $\widehat{A}_2$ be observables acting respectively on $\mathcal{H}_1$ and $\mathcal{H}_2$. Their tensor product $\widehat{A}_1 \otimes \widehat{B}_2$ is the observable acting on $\mathcal{H}$, defined by following relation:

$$[\widehat{A}_1 \otimes \widehat{A}_2]\ [|\psi_1\rangle \otimes |\psi_2\rangle] \ = \ [\widehat{A}_1\,|\psi_1\rangle] \otimes [\widehat{A}_2\,|\psi_2\rangle] \text{ with } \psi_1 \in H_1 \text{ and } \psi_2 \in H_2 \tag{1.14}$$

Any of these observables can be formed by a linear combination of tensorially multiplied Pauli matrices:

$$[\widehat{A}_1 \otimes \widehat{A}_2] = \sum_{i,j=0}^{3} s_{ij}\ \widehat{\sigma_i} \otimes \widehat{\sigma_j} \tag{1.15}$$

with $\widehat{\sigma}_0 = 1;\ \widehat{\sigma}_1 = \widehat{\sigma}_x;\ \widehat{\sigma}_2 = \widehat{\sigma}_y;\ \widehat{\sigma}_3 = \widehat{\sigma}_z;\ s_{i,j}\ \in \mathbb{C}$.

Using this formalism of the tensor product a projector can be defined similarly to the single qubit case. Here the P_{HV} projector is shown:

$$P_{HV} = P_H \otimes P_V = \frac{1}{2}(1 + \widehat{\sigma}_z) \otimes \frac{1}{2}(1 - \widehat{\sigma}_z) \tag{1.16}$$

For example [10], the correlation of $\widehat{\sigma}_z \otimes \widehat{\sigma}_z$ and a state $|\Psi(a_{HH}, a_{HV}, a_{VH}, a_{VV})\rangle$ is therefore given by:

$$\begin{aligned}
K_{zz} &= \langle\Psi(a_{HH}, a_{HV}, a_{VH}, a_{VV})|\widehat{\sigma}_z \otimes \widehat{\sigma}_z|\Psi(a_{HH}, a_{HV}, a_{VH}, a_{VV})\rangle = \\
&= \frac{1}{4}(\langle\Psi|[1 + \widehat{\sigma}_z] \otimes [1 + \widehat{\sigma}_z]|\Psi\rangle - \langle\Psi|[1 + \widehat{\sigma}_z] \otimes [1 - \widehat{\sigma}_z]|\Psi\rangle - \\
&- \langle\Psi|[1 + \widehat{\sigma}_z] \otimes [1 - \widehat{\sigma}_z]|\Psi\rangle + \langle\Psi|[1 - \widehat{\sigma}_z] \otimes [1 - \widehat{\sigma}_z]|\Psi\rangle) = \\
&= \langle\Psi|P_H \otimes P_H|\Psi\rangle - \langle\Psi|P_H \otimes P_V|\Psi\rangle - \langle\Psi|P_V \otimes P_H|\Psi\rangle + \langle\Psi|P_V \otimes P_V|\Psi\rangle = \\
&= |a_{HH}|^2 - |a_{HV}|^2 - |a_{VH}|^2 + |a_{VV}|^2 = p_{HH} - p_{HV} - p_{VH} + p_{VV},
\end{aligned} \tag{1.17}$$

where p_{ij} ($\{ij\} \in \{H, V\}$) are the probabilities of occurrence in the $|H/V\rangle$ basis. A correlation value $K_{zz} = +1$ implies that the measurement outcome of each qubit is always equal, i.e. the state is correlated in this basis. An uncorrelated result is thus expressed by $K_{zz} = 0$, while an anticorrelated result is associated with $K_{zz} = -1$.

1.1.3 Bell States and entanglement

In this section, different entangled states are considered more precisely. For a two-photon vector space the following entangled orthogonal states can be defined - the Bell states:

$$\begin{aligned} |\phi^+\rangle &= \frac{1}{\sqrt{2}}(|HH\rangle + |VV\rangle) \\ |\phi^-\rangle &= \frac{1}{\sqrt{2}}(|HH\rangle - |VV\rangle) \\ |\psi^+\rangle &= \frac{1}{\sqrt{2}}(|HV\rangle + |VH\rangle) \\ |\psi^-\rangle &= \frac{1}{\sqrt{2}}(|HV\rangle - |VH\rangle). \end{aligned} \tag{1.18}$$

The mathematical property that they cannot be produced by a tensor product has profound consequences in the physical context of quantum mechanics [17]. Here some properties rising from this effect are demonstrated:

1. Each Bell state can be converted to any other Bell state by a unitary transformation on one of the two qubits [10]:

$$|\phi^+\rangle = (1 \otimes \widehat{\sigma}_z)\,|\phi^-\rangle = (1 \otimes \widehat{\sigma}_x)\,|\psi^+\rangle = (1 \otimes \widehat{\sigma}_y)\,|\psi^-\rangle \tag{1.19}$$

   except a global phase. So a transformation on only one qubit of an entangled state, changes the complete state. This will become even more obvious, if the new state is rotated back to the original one by a transformation on the other qubit, for example:

$$(\widehat{\sigma}_x \otimes 1)\,|\phi^+\rangle = |\psi^+\rangle \tag{1.20}$$

2. Entangled states are correlated in more than one basis in contrast to separable states. For them correlation can only be observed along one two-photon basis, whereas in other bases they are uncorrelated.
   A reverse result occurs, if one considers local correlations $\widehat{\sigma}_i \otimes 1$ (i $\in$ {X,Y,Z}). They vanish for entangled states making it impossible to determine the single photon state. In contrast to separable states, wherefore one local correlation is unequal to 0. This allows to specify the single qubit state with 100% certainty. For example:

$$\begin{aligned} &\langle HH|\widehat{\sigma}_z \otimes 1|HH\rangle = 1 \\ &\langle \phi^+|\widehat{\sigma}_i \otimes 1|\phi^+\rangle = 0 \quad \text{with i} \in \{x, y, z\} \end{aligned} \tag{1.21}$$

   These properties give rise to violation of local realism, because for a local realistic theory the measurement of one particle, which is spatial separated from another one, does not influence the second particle. This will be described more precisely in the next section.

1.2 EPR paradox and Bell's inequality

1.2.1 EPR paradox

The usual interpretation of quantum mechanics leads to intrinsic random results for measurements. Therefore, Einstein was convinced that "the description of reality as given by

a wave function is not complete" [7]. Especially the uncertainty principle, which prohibits the possibility to measure two non-commuted operators with unlimited accuracy, irritated Einstein. He assumed that it should be possible to find a theory with hidden parameters explaining the results of quantum theory, but still fulfilling the requirements of a deterministic and local theory. So in 1935 Einstein, Podolski and Rosen (EPR) published a gedankenexperiment which should demonstrate the existence of hidden variables and the incompleteness of quantum mechanics. The basic assumptions formulated in the version of Bohm and Aharonov can be summarized as follows:

1. **Completeness:** "Every element of the physical reality must have a counterpart in the physical theory." [7]
2. **Realism:** "If, without in any way disturbing a system, we can predict with certainty (i.e., with probability equal to unity) the value of a physical quantity, then there exists an element of physical reality corresponding to this physical quantity." [7]
3. **Locality:** It is possible to separate physical systems, so that they don't influence each other as the cannot transmit information with v > c.
4. **Perfect Anticorrelations:** If you measure the spin of both particles in the same direction, you will get opposite results.

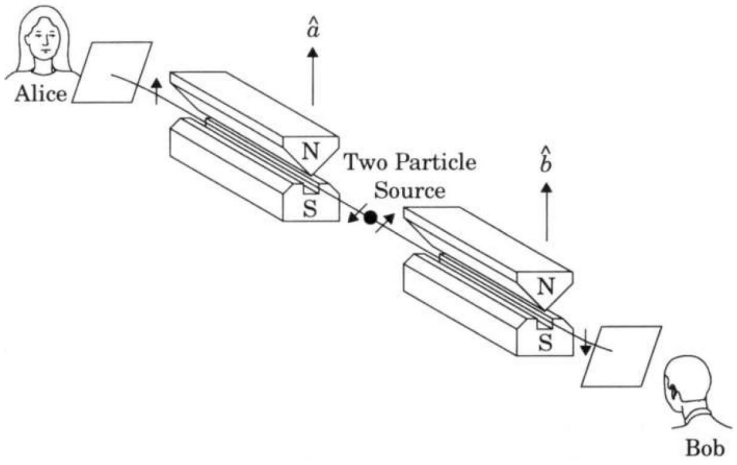

Figure 1.2: Stern-Gerlach experiment for the determination of spins of two particles (from [3])

They argued as follows [20]: Two spin $\frac{1}{2}$ particles in an entangled state $|\psi\rangle = \frac{1}{\sqrt{2}}(|\uparrow\downarrow\rangle + |\downarrow\uparrow\rangle)$ (see the Bell state ψ^+ of Eqn. 1.18) are considered and fly away in different directions. By a spin measurement of particle A, e.g. along the X direction, the spin of particle B can also be determined along this direction.
Due to assumption 3. this measurement does not influence particle B and due to 4, the spin of particle B is inverse to particle A. So the spin of particle B is known and due to 2, it is an element of physical reality. It would also be possible to measure the spin of particle B e.g. along the Z direction and thus, this spin is also an element of physical reality. This result contradicts the uncertainty principle. Therefore, hidden variables must exist which

determine these measurement results being necessary to extend quantum mechanics to a complete local and realistic theory.
Bohr countered these arguments, that knowing the state of a whole system, does not necessarily mean that its parts can be determined, as they are not in a defined state. Furthermore, after the measurement of one particle the result of the other one will instantaneously be known. This is a contradiction to the locality assumption when the two particles are spatially separated. So Bohr's version explained the problem by rejecting the principles of local realism.
The EPR-paradox became more a philosophical problem during nearly the next 30 years (see also [18]), because no possibility was known to measure a difference between the predictions of quantum mechanics or of hidden variable theory.

1.2.2 Bell's - CHSH inequality

In 1964 Bell found a solution for this problem [4]. He showed that it is possible for certain measurements to get different results between a quantum mechanical and a hidden variable theory calculation. In other words, one can find bounds between a local, deterministic model and the nonlocal, non realistic prediction of quantum mechanics.
In contrast to the original proposal of Bell, in this experiment a similar inequality is used [13]. It does not require perfect correlations and therefore, is better adapted to realistic experimental conditions: the Clauser, Horne, Shimony and Holt (CHSH) inequality. For an exact derivation see [5]. Here only a short conclusion is given.

Local realistic description
We consider the setup as described for the EPR-paradox. Let λ be set of hidden variables (w.l.o.g. it should be one dimensional) and p(λ) its probability distribution determining the measurement results for any possible measurement setting. In contrast, the quantum mechanical probabilistic measurement results are explained by the lack of knowledge of the statistical distribution p(λ). Two different measurement outcomes are provided for one particle by (A(a,λ), A(a',λ)) and for the other one by (B(b,λ), B(b',λ)), where a, a' and b, b' are adjustable apparatus parameters. The measurement results are deterministic functions, i.e. they depend on λ and their spectrum is $\{\pm 1\}$.The principle of locality requires A(a,λ), A(a',λ) being independent of B(b,λ), B(b',λ) and vice versa. This is ensured by a spacial separation of the measurement apparatuses. Consequently, the correlation value E of the measurements factorizes as

$$E(a,b) = \int d\lambda \; p(\lambda) \; A(a,\lambda) \; B(b,\lambda) = E(a) \cdot E(b). \tag{1.22}$$

Making use of the constraints of A and B, an equality for the different settings can be

defined [17]. For a single measurement it is given by:

$$\begin{aligned} &|A(a,\lambda)B(b,\lambda) - A(a,\lambda)B(b',\lambda)| + |A(a',\lambda)B(b,\lambda) + A(a',\lambda)B(b',\lambda) = \\ &= \underbrace{|A(a,\lambda)}_{\pm 1}\underbrace{(B(b,\lambda) - B(b',\lambda))|}_{\begin{matrix}0\\ \pm 2\\ 0\end{matrix}} + \underbrace{|A(a',\lambda)}_{\pm 1}\underbrace{(B(b,\lambda) + B(b',\lambda)|}_{\begin{matrix}+2\\ 0\\ -2\end{matrix}} = 2 \end{aligned} \tag{1.23}$$

Using the definition of the correlation value and the inequality $|\int f(x)dx| \leq \int |f(x)|dx$ the CHSH inequality can be derivated:

$$S(a,a',b,b') = |E(a,b) - E(a,b')| + |E(a',b) + E(a',b')| \leq 2 \tag{1.24}$$

Quantum violation

In quantum mechanics, the correlation functions can be calculated as described in the following [23]. In the example, we use the maximally entangled state (see Eqn. 1.18)

$$|\phi^+\rangle = \frac{1}{\sqrt{2}}(|HH\rangle + |VV\rangle). \tag{1.25}$$

The maximum violation of the CHSH inequality occurs for certain measurement settings. For θ and ϕ in the observable $\widehat{\sigma}_{\theta,\phi}$ of the Eqn.1.5 the values below allow to observe a maximal violation:

$$\begin{aligned} &\phi = 0 \text{ (for all measurements)} \\ &\theta_1 = \alpha = \frac{\pi}{2}\ ;\ \theta_2 = \alpha' = 0\ ;\ \theta_3 = \beta = \frac{\pi}{4}\ ;\ \theta_4 = \beta' = -\frac{\pi}{4} \end{aligned} \tag{1.26}$$

Note that a value of $\phi = 0$ corresponds to a rotation in the equatorial plane of the Bloch sphere and therefore, only linear polarized light is necessary to show the violation of the CHSH inequality (see figure 1.1).

The correlation functions can be calculated as follows:

$$E_{QM}(\alpha,\beta) = \langle\phi^+|\widehat{\sigma}_{\alpha,0} \otimes \widehat{\sigma}_{\beta,0}|\phi^+\rangle = \cos(\alpha - \beta) \tag{1.27}$$

Using the above angles they result in:

$$E_{QM}(\alpha,\beta) = E_{QM}(\alpha',\beta) = E_{QM}(\alpha',\beta') = -E_{QM}(\alpha,\beta') = \cos(\pi/4) = \frac{1}{\sqrt{2}} \tag{1.28}$$

In the next step these values can be inserted in Eqn. 1.24 and a violation of the classical limit is observed:

$$S_{QM}(\alpha,\alpha',\beta,\beta') = 2\sqrt{2} > 2. \tag{1.29}$$

Please note that the correlation function is by historical reasons denoted by E here. In the following, we will come back to denoting a correlation by the letter K.

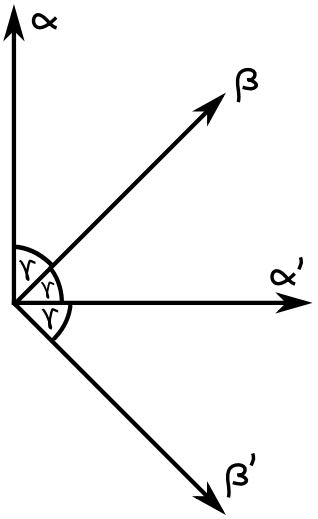

Figure 1.3: Illustration of the angles corresponding to maximal violation of the CHSH inequality where $\gamma = \frac{\pi}{4}$ (from [19]).

The first experimental test of Bell's (CHSH) inequality was done by Friedman and Clauser in 1972 [8] and subsequently most prominently by A. Aspect et al. in 1981 [2]. All experiments so far affirm the quantum mechanical predictions up to the closure of different loopholes. Two major loopholes exist [21], which still make the local realistic description of the experiments possible. The first one is the so called locality loophole. It occurs, whenever the communication between the measurement settings of the two observers cannot be excluded before completing the actual measurement process. In experiments, this loophole can be ruled out by achieving a space-like separation of the two particles with respect to their measurement time. In 1998 the first experiment which violated a Bell's inequality under strict locality conditions has been performed by Weihs et al. [24] and was improved further by Scheidl et al. in 2010 [15], who separated the two observers by a distance of 144 km.
However, in all these experiments the detection efficiencies of the entangled photons were too low to close the so called detection loophole. This describes the possibility that the whole ensemble may behave according to local realism, while the detected particles do not, because they are not representative for the whole ensemble. A Bell test, which eliminated successfully this loophole, was performed with a pair of entangled beryllium ions. But in this system the separation of the ions by distance of about $3\,\mu$m gives no chance to close the locality loophole [23]. Thus, the local realistic description is not ruled out completely and a final test of Bell's inequality has to be accomplished yet.

1.3 Density operator

1.3.1 Mixed states

So far, we have only considered pure states, which are represented by a state vector. However, such a state cannot be produced perfectly in an experiment. For example, because of uncontrollable, systematical changes of the state only incomplete information about the state can be extracted and therefore only probability statements are possible. In the density operator formalism the state can be described following the axioms of classical probability calculation. The density operator of any state is defined by [6]:

$$\rho = \sum_i p_i \left|\phi_i\right\rangle \left\langle\phi_i\right| \text{ with } \sum_i p_i = 1 \text{ and } \left|\phi_i\right\rangle \text{being pure states} \tag{1.30}$$

If the information of a state is incomplete, the p_i are statistically distributed and the state is a statistical mixture over pure states. So it is called a mixed state.
The general characteristics of a density operator are described by:

- Probability conservation: Tr(ρ)=1
- Positive semi-definite which is necessary for a physical state: $\lambda_i \geq 0$, $\forall$ i (λ_i are the eigenvalues of ρ)
- Expectation value for an operator A: $\langle A\rangle = \langle\psi|A|\psi\rangle = Tr(\rho A)$

The density operator can be written as a matrix for a given orthonormal basis:

$$\rho_{ij} = \langle i|\rho|j\rangle \tag{1.31}$$

where i, j $\in$ $\{1, 2, ..., N\}$ with the basis vectors $|i\rangle$ and $|j\rangle$. Here the $|H\rangle$, $|V\rangle$ basis is used and therefore, the basis vectors of a two qubit state are given in Eqn.1.12: $|1\rangle = |HH\rangle$; $|2\rangle = |HV\rangle$; ... The density matrix can also be expressed through the Pauli spin matrices (see chapter 1.1.1 and [9]). For a single qubit it is given as follows:

$$\rho = \frac{1}{2}\sum_{i=0}^{3} s_i \,\widehat{\sigma}_i \tag{1.32}$$

Extending this formalism to two qubits (see 1.1.2):

$$\rho = \frac{1}{2^2}\sum_{i,j=0}^{3} s_i \,\widehat{\sigma}_i \otimes \widehat{\sigma}_j \tag{1.33}$$

The measurement of a density matrix through quantum tomography is the second part of this lab course. Therefore, the physical interpretation of the matrix elements ρ_{ij} will be explained shortly. The example of the single qubit state $\rho_{RR} = |R\rangle\langle R|$ is presented to illustrate the differences between the diagonal and non-diagonal elements of a density matrix expressed in the $|H\rangle$, $|V\rangle$ basis:

$$\rho_{RR} = \frac{1}{2}\begin{pmatrix} 1 & -i \\ i & 1 \end{pmatrix} = \frac{1}{2}(1 + \widehat{\sigma}_y) \tag{1.34}$$

- The diagonal element ρ_{ii} represents the probability for observing the system in the basis state $|i\rangle$. Thus, it is called the population of the state $|i\rangle$ and is always a positive real number.
- The non-diagonal element ρ_{ij} describes the quantum coherences between the basis states $|i\rangle$ and $|j\rangle$. It does not vanish, when the state $|\psi\rangle$ is a coherent linear superposition of $|i\rangle$ and $|j\rangle$. More precisely, for product states a set of basis transformations exists, acting on the subspaces $|i\rangle$ and $|j\rangle$, such that ρ takes diagonal form in the new product basis. Consequently, the non-diagonal elements have no invariant meaning for product states. Nevertheless, no product basis describes an entangled state and therefore ρ of an entangled state can never be diagonal in such a basis. So non-diagonal elements only occur within quantum theory. They are called coherences or quantum correlations and are complex numbers [14].

1.3.2 Derivations of the density operator

Many quantities which characterize a quantum state can be calculated out of a density matrix. Here some of these will be presented.

1. **Purity:**
   The Purity describes, if a state is pure or mixed:

   $$\mathcal{P}(\rho) = Tr(\rho^2) \tag{1.35}$$

   It is 1 for pure states and 1/N, where N is the dimension of the state, for totally mixed states [16].

2. **Fidelity:**
   Uhlmann presented the Fidelity in 1976 [22]. It measures the state overlap between two states ρ and σ:

   $$\mathcal{F}(\rho, \sigma) = (Tr(\sqrt{\sqrt{\sigma}\rho\sqrt{\sigma}}))^2 \tag{1.36}$$

   It can be used to quantify how well a experimental imperfect state ρ resembles another general state σ. In our case the reference state is pure and therefore the fidelity simplifies to [1]:

   $$\mathcal{F}(\rho, \sigma) = Tr(\sigma\rho) \tag{1.37}$$

3. **PPT-criterion and negativity:**
   The Positive Partial Transpose (PPT) criterion allows to verify the entanglement by prior knowledge of the density matrix [10]. A separable state ρ can be written in the density matrix formalism:

$$\rho_{sep} = \sum_i p_i \, \rho_i^a \otimes \rho_i^b \tag{1.38}$$

   The partial transpose of a matrix is defined by:

$$\rho^{T_a} = \sum_i p_i \, (\rho_i^a)^t \otimes \rho_i^b \tag{1.39}$$

   Peres-Horodecki Theorem for a two qubit Hilbert space:

$$\rho \text{ separable} \quad \Leftrightarrow \quad \rho^{T_a} \geq 0 \tag{1.40}$$

   For example,

$$\rho_{HH} = |HH\rangle \langle HH| \overset{PT}{\rightarrow} \rho_{HH}^{T_a} = |HH\rangle \langle HH| \tag{1.41}$$

   is again a physical state with $\rho_{HH}^{T_a} \geq 0$. But, if we choose

$$\begin{aligned} \rho_{\phi^+\phi^+} = |\phi^+\rangle \langle \phi^+| &= \frac{1}{2}(|HH\rangle \langle HH| + |HH\rangle \langle VV| + |VV\rangle \langle HH| + |VV\rangle \langle VV|) \\ \overset{PT}{\rightarrow} \rho_{\phi^+\phi^+}^{T_a} &= \frac{1}{2}(|HH\rangle \langle HH| + |VH\rangle \langle HV| + |HV\rangle \langle VH| + |VV\rangle \langle VV|) \end{aligned} \tag{1.42}$$

   it can be shown, that the partial transpose density matrix has a negative eigenvalue of $-\frac{1}{2}$, i.e. $\rho_{\phi^+\phi^+}^{T_a} < 0$. So the PPT-criterion is useful a test of the entanglement.

4. **Entanglement witness**
   An entanglement witness provides another possibility to detect entanglement and defines a probability for having generated the desired state [19].

   Terhal Theorem:

   If ρ is entangled, then there exists a Hermitian operator W acting on $\mathcal{H}_1 \otimes \mathcal{H}_2$ such that:

$$Tr(W\rho) < 0 \text{ and } Tr(W\rho_{sep}) \geq 0 \tag{1.43}$$

   for all positive semi definite density matrices ρ_{sep}.

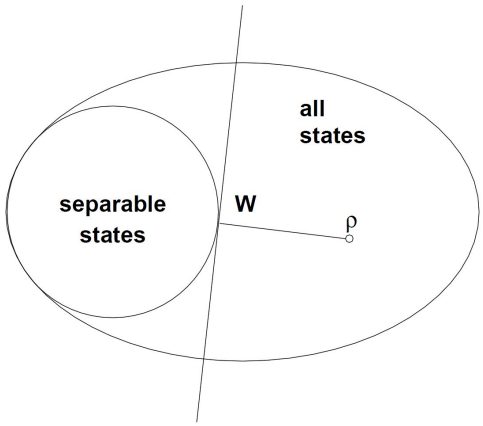

Figure 1.4: Schematic representation of the Hilbert space and a witness operator (from [19]).

Figure 1.4 illustrates this theorem. A hyperplane separating the set of all separable density matrices on $\mathcal{H}_1 \otimes \mathcal{H}_2$ can be defined from the point ρ. The hyperplane consists of a set of density matrices, κ , and its normal vector W is defined by $\mathrm{Tr}(W\kappa) = 0$. So the space is divided into two areas: In the first $\mathrm{Tr}(W\rho)$ is < 0 and all detected entangled states are located here. In the second $\mathrm{Tr}(W\rho)$ is ≥ 0, where separable and non detected entangled states can be situated. As a consequence, ρ is an entangled state, if $\mathrm{Tr}(W\rho)$ is < 0 and the operator W is called entangled witness.

A witness is called optimal if it reveals a specific state with 100% probability, but other states can be detected, too.

For our experimental situation where we produce nearly a pure state, e.g. ϕ^+, it is always possible to find an optimal witness operator. In this model experimental conditions are considered by introducing noise. It is represented by a mixed state χ and the effectively produced state is described by:

$$\rho = p \left|\phi^+\right\rangle \left\langle\phi^+\right| + (1-p)\chi \tag{1.44}$$

where p is the probability of having produced ϕ^+. It can be shown, that a optimal witness operator W, which fulfills the Terhal Theorem, is given by:

$$W = \left(\left|e_{min}\right\rangle \left\langle e_{min}\right|\right)^{T_a} \tag{1.45}$$

where $\left|e_{min}\right\rangle$ is the eigenvector of ρ^{T_a} corresponding to the eigenvalue $\lambda_{min} < 0$.

Calculating this explicitly for the Bell states one finds following witness operators:

$$\begin{aligned}
W(\phi^+) &= \frac{1}{2}(-|HH\rangle\langle VV| - |VV\rangle\langle HH| + |HV\rangle\langle HV| + |VH\rangle\langle VH|) \\
W(\phi^-) &= \frac{1}{2}(\ \ |HH\rangle\langle VV| + |VV\rangle\langle HH| + |HV\rangle\langle HV| + |VH\rangle\langle VH|) \\
W(\psi^+) &= \frac{1}{2}(\ \ |HH\rangle\langle HH| + |VV\rangle\langle VV| - |HV\rangle\langle VH| - |VH\rangle\langle HV|) \\
W(\psi^-) &= \frac{1}{2}(\ \ |HH\rangle\langle HH| + |VV\rangle\langle VV| + |HV\rangle\langle VH| + |VH\rangle\langle HV|)
\end{aligned} \tag{1.46}$$

Assuming that χ is white noise, the probability p can be calculated as follows:

$$p = \frac{1}{3}(1 - 4\,\mathrm{Tr}(W\rho)) \tag{1.47}$$

It can be considered as a measure for the entanglement quality of the state for which the witness was optimized.

Notation:
A Bell inequality is also an entanglement witness, but it can be understood as a witness which is not optimized. For the Bell states this means no difference, because they maximally violate a Bell inequality. However, there exist non-separable states which don't violate the Bell inequality, but their entanglement can be detected by a witness [19].

2 Experimental setup

The theoretical essentials were introduced so far and in the next step the experimental implementation used in our case should be explained. The polarization degree of freedom is probable the most illustrative and most popular encoding of entanglement. Here we address the question of how to prepare and analyze a polarization-entangled state?
Figure 2.1 shows an overview of the experimental setup. It is split into two parts: First the generation of entangled photons in figure 2.1(a) and second the polarization analysis and the detection system in figure 2.1(b). These parts will be explained in detail in the following sections.

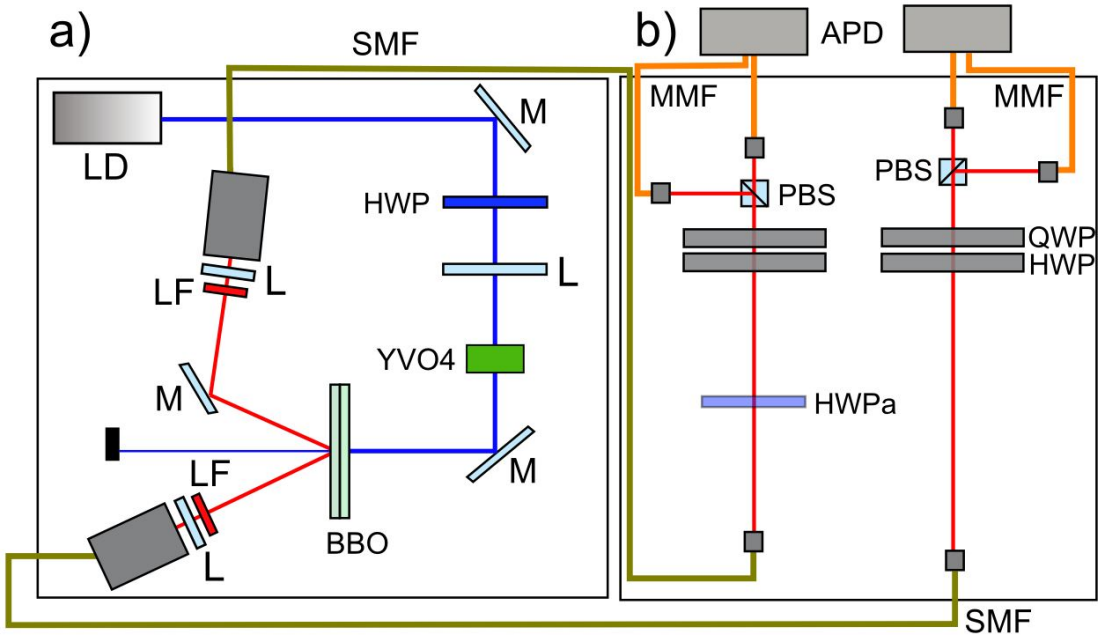

Figure 2.1: Schematic setup: laser diode (LD), longpass filter (LF), half-wave plate (HWP), lens (L), compensation crystal (YVO4), mirror (M), SPDC crystal (BBO), single-mode fiber (SMF), additional half-wave plate (HWPa), polarization beam splitter (PBS), multi-mode fiber (MMF),single photon detectors (APD).

2.1 Generation of the entangled photons

The pump laser - a UV laser diode

In the experiment a blue laser diode is used which produces vertical (V) polarized photons at nominal wavelength of λ= 403 nm. It is driven with a supply current of 60 mA for which the optical output power is 30 mW. The coherence length of the laser diode is in the range of some μm [16]. Using this laser, photon pairs produced by SPDC can be created .

SPDC with two BBO crystals

A single pump photon of the laser can be split up into a photon pair. Here we make use of a parametric process in nonlinear crystals: the Spontaneous Parametric Down Conversion (SPDC) [17]. The process can be explained by the presence of an electromagnetic field $\vec{E}$ in a crystal which induces a polarization $\vec{P}$ of the medium. In an anisotropic crystal, whereupon the relation between $\vec{P}$ and $\vec{E}$ depends on the direction of the latter, the components P_i of the polarization can be expressed in a power series

$$P_i = \epsilon_0 \sum_j \chi_{ij}^{(1)} E_j + \epsilon_0 \sum_{j,\,k} \chi_{ijk}^{(2)} E_j E_k + ... \tag{2.1}$$

with i, j, k $\in$ {X,Y,Z} and ϵ_0 is the vacuum permittivity. $\chi_{ij}^{(1)}$ is the susceptibility tensor of the medium and $\chi_{ijk}^{(2)}$ its pendant of second order. Their typical strengths are in the range of $\chi_{ij}^{(1)} \approx 1$, $\chi_{ijk}^{(2)} \approx 10^{-10}$ cm/V [25]. So the second order can be neglected for weak fields, but a strong pump field is sufficient to generate a measurable result. In this picture the SPDC corresponds to the generation of two fields, called signal and idler, with the frequencies ω_s and ω_i out of one field with the frequency ω_p.
However, the SPDC can only be understood quantum mechanically as it represents a spontaneous process. In the photon picture it can be seen as the spontaneous conversion of a pump photon with energy $\hbar\omega_p$ and momentum $\hbar\vec{k}_p$ into two photons with energies $\hbar\omega_s$, $\hbar\omega_i$ and momenta $\hbar\vec{k}_s$, $\hbar\vec{k}_i$ [16].
In the SPDC process the energy and momentum conservation must hold:

$$\omega_p = \omega_s + \omega_i \tag{2.2}$$

$$\vec{k}_p = \vec{k}_s + \vec{k}_i \tag{2.3}$$

A more detailed quantum mechanical derivation of this process can be found e.g. in [12]. Due to the birefringence of the optical material two types of SPDC can be distinguished, when the pump beam is extraordinarily polarized:[1]

- **Type I**: Both down converted photons are ordinarily polarized regarding to the principal axis of the crystal.
- **Type II**: Signal and idler photons are orthogonally polarized, i.e. one ordinarily the other one extraordinarily.

For exploiting the correlations in the polarization degree of freedom, two type I nonlinear crystals made of Beta-barium borate (BBO) are used in this experiment [21]. These crystals are optically contacted, 1mm thin and their optical axes lie in mutually perpendicular planes. For example, the optical axis of the first crystal is oriented along V, while for the second crystal it is orientated along H. Therefore, SPDC with a V polarized pump

[1] Extraordinarily polarized means the polarization vector lies in the plane spanned by the principal axis of the crystal and the wave vector of the pump photon, in contrast to ordinarily polarized where the polarization vector is normal to this plane.

beam occurs only in the first crystal, whereas with an H polarized pump it occurs only in the second crystal. By pumping the crystal with + (45° regarding to the H and V direction) polarized light the probability that a pump photon is down converted in either crystal is equal. So an additional optical element (in our case a half-wave plate, see also section 2.2) is needed, which rotates the V polarized laser photons to + polarization.

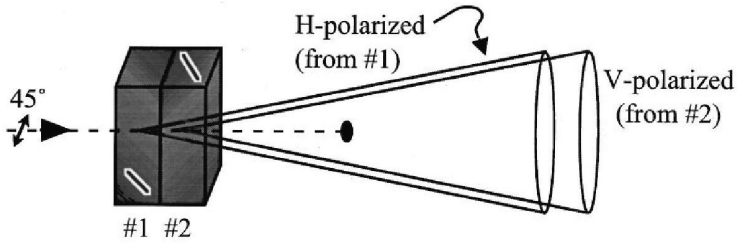

Figure 2.2: Two identical type I down-conversion crystals, oriented at 90° with respect to each other and the emission cones of the H and V polarized photons are illustrated (from [11]).

Momentum conservation implies that the down converted photons are emitted along symmetric cones around the pump beam direction. Furthermore, it imposes that correlated photon pairs can only be observed at diametrically opposed position of the emission cones. In this double crystal type I source the H polarized photons lie on one cone and the V polarized photons on the other cone [11]. Ideally the two cones and thereby, two photons in the $|HH\rangle$ or $|VV\rangle$ state overlap coherent at every point. To realize this experimentally, i.e. to prepare an entangled state out of the two photons, additional optical elements are needed. They will be described in the next sections.

Compensation and phase adjustment

Because of birefringence and chromatic dispersion in the optical material of the BBO crystals a temporal separation between the ordinarily and extraordinarily polarized photons arises. If the temporal separation is larger than the coherence time of the laser, no coherence between both photon pairs will be observed, as the photons can be distinguished in principle by their detection time. To solve this problem an additional compensation crystal is required. In this experiment a Yttrium Vanadate (YVO_4) crystal with an optical axis orientated parallel to the pump laser beam is introduced [14]. A variation of the optical path length and therefore a phase between the H and V components of the pump light can be implemented by tilting the crystal. So the time overlap between two photons of the SPDC processes can be adjusted and a high-quality entangled state can be produced.

Selection of two spatial modes

For the observation of a high quality entangled state the following points have to be considered, too. Lenses coupling the photons into single mode fibers are placed at diametrically opposed points of the emission cones. Otherwise no simultaneously detected photons will be observed, because they are emitted from different down conversion processes. For a good quality the two couplers collect the same amount of photons from both crystals [14].

Finally, spectral selection is achieved by introducing filters in each spatial selected mode centered around 805 nm and a bandwidth of 6 nm. They are necessary, as the bandwidth of the down conversion photons is too wide to keep them indistinguishable due to different phases acquired in the fibers and in the optical components used to prepare and analyze the entangled state. But the disadvantage of these filters is the considerable reduction of the amount of produced photon pairs.

Preparation of Bell states

Like described above the source produces $|HH\rangle$ or $|VV\rangle$ photon states. After the alignment of the additional optical components these pairs are in a coherent superposition and consequently the photons will automatically create the state:

$$\begin{aligned} |\phi\rangle &= |H, A, E_1\rangle \otimes |H, B, E_2\rangle + \mathrm{e}^{i\phi} |V, A, E_1\rangle \otimes |V, B, E_2\rangle = \\ &= |A, B\rangle \ |E_1, E_2\rangle \ (|HH\rangle + \mathrm{e}^{i\phi} |VV\rangle) \end{aligned} \tag{2.4}$$

"A" and "B" correspond to the two spatial selected modes and E_1 and E_2 are the two energies of these modes. For a relative phase $\phi = 0$ (π) the Bell state $|\phi^+\rangle$ ($|\phi^-\rangle$) occur. The other two Bell states $|\psi^+\rangle$ and $|\psi^-\rangle$ can be prepared by adding a half-wave plate in one of the modes to exchange H and V polarization (for a detailed explanation see 2.2) As a result of this process, two photonic qubits which differ in no other degree of freedom than their spatial mode and polarization can be generated very well (for details see [21]). The analysis of such a state will be explained in the following.

2.2 Polarization analysis and the detection system

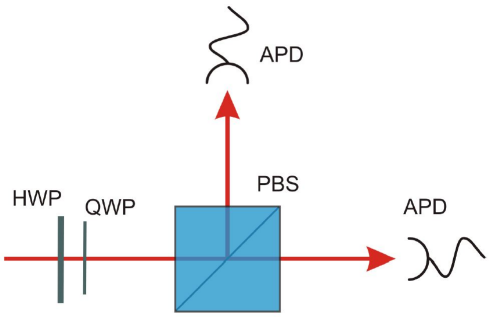

Figure 2.3: The polarization analysis as used in the experiment is depicted (from [10]).

Figure 2.3 shows the polarization analysis which is installed in each of the two modes. Consequently, each photon is measured independently. It consists of a half-wave plate (HWP) and a quarter-wave plate (QWP) followed by a polarization beam splitter (PBS). The PBS transmits H polarized and reflects V polarized light. In other words, the PBS implemented a projection measurement onto the eigenvectors of σ_z, $|H\rangle$ and $|V\rangle$. To measure another polarization direction of the incoming photon, i.e. another vector of the Hilbert space, an additional rotation of the polarization direction onto H (or V) is necessary. This rotation is given by a HWP and a QWP.

The function of a HWP and QWP can be summarized in the following way (see also [1]). Wave plates are implemented by zero-order, uniaxial birefringent crystals. HWP introduces a relative phase shift of π, between the ordinary and extraordinary polarization modes with respect to the orientation of the crystals. Hence, it rotates the polarization direction of linear polarized light by an arbitrary angle, i.e. in the equatorial plane of the Bloch sphere (see figure 1.1). Accordingly, QWP introduces a relative phase shift of $\frac{\pi}{2}$ and changes linear polarized light to circular and vice versa. In the experiment the angles α_{HWP} and α_{QWP} between the vector of horizontal polarization and the principal axis of the wave plates can be set by a rotation of the wave plates (see section 2.3).
Note: When the HWP is turned to α_{HWP}, it will rotate the polarization by -2 α_{HWP}, in contrast the QWP turns the polarization exact by α_{QWP} .
Accordingly, it is possible to analyze any point on the Bloch sphere with these two wave plates. For example [17], adjusting the HWP to $\alpha_{HWP} = -\frac{\pi}{8}$ and the QWP to $\alpha_{QWP} = 0$ an incoming photon in one of the eigenstates of $\widehat{\sigma}_x$, $|+\rangle$ or $|-\rangle$, is rotated to $|H\rangle$ or $|V\rangle$. In general, the wave plates implement the following transformation which rotates the eigenvectors of $\widehat{\sigma}_{\theta,\phi}$ onto the ones of $\widehat{\sigma}_z$ [25] :

$$\widehat{\sigma}_z = (\mathrm{QWP}(\alpha_{QWP})\,\mathrm{HWP}(\alpha_{HWP}))\widehat{\sigma}_{\theta,\phi}(\mathrm{QWP}(\alpha_{QWP})\,\mathrm{HWP}(\alpha_{HWP}))^{\dagger} \tag{2.5}$$

$$\begin{aligned} \text{with} \quad \mathrm{HWP}(\alpha_{HWP}) &= \begin{pmatrix} cos(2\alpha_{HWP}) & sin(2\alpha_{HWP}) \\ sin(2\alpha_{HWP}) & -cos(2\alpha_{HWP}) \end{pmatrix} \\ \mathrm{QWP}(\alpha_{QWP}) &= \begin{pmatrix} cos^2(\alpha_{QWP}) - isin^2(\alpha_{QWP}) & (1+i)cos(\alpha_{QWP})sin(\alpha_{QWP}) \\ (1+i)cos(\alpha_{QWP})sin(\alpha_{QWP}) & -icos^2(\alpha_{QWP}) + sin^2(\alpha_{QWP}) \end{pmatrix} \end{aligned} \tag{2.6}$$

What angles α_{HWP} and α_{QWP} are need to rotate a photon initially at $|R\rangle$ or $|L\rangle$ to $|H\rangle$ or $|V\rangle$?

So far, single photon projections were described. For two photons, projections onto the two qubit Hilbert space have to be associated to experimental values. The measurement of coincidences between two output modes corresponding to a projection onto HH, HV, VH or VV. A coincidence event means that we register two 'clicks' in two different detectors within a time interval of 10 ns. The two outputs of each PBS are coupled into multi-mode fibers which directed to single photon detectors (APDs). Their single photon sensitivity allows to trigger a single electrical pulse, when a photon is absorbed in the active semiconductor material. Two electrical pulses from different detectors are combined to measure coincidences [16].
The advantage of using a polarization analysis with two detectors in each mode is the possibility to detect simultaneously the four coincidence rates C_{HH}, C_{HV}, C_{VH}, C_{VV}. These four rates allow to determine the normalization of a state for each measurement setting and the relative frequencies can be calculated out of them:

$$f_{ij} = \frac{C_{ij}}{\sum_{i,\,j} C_{ij}} (i,j \in \{H,V\}) \tag{2.7}$$

They can be associated to the probabilities p_{ij} of Eqn. 1.17. Therefore, the experimental measured correlations are given by:

$$K_{ij}^{ex} = f_{HH} - f_{HV} - f_{VH} + f_{VV} =$$

$$= \frac{C_{HH}(\alpha_{HWP},\alpha_{QWP}) - C_{HV}(\alpha_{HWP},\alpha_{QWP}) - C_{VH}(\alpha_{HWP},\alpha_{QWP}) + C_{VV}(\alpha_{HWP},\alpha_{QWP})}{C_{HH}(\alpha_{HWP},\alpha_{QWP}) + C_{HV}(\alpha_{HWP},\alpha_{QWP}) + C_{VH}(\alpha_{HWP},\alpha_{QWP}) + C_{VV}(\alpha_{HWP},\alpha_{QWP})} \tag{2.8}$$

with i, j $\in$ {X,Y,Z}. A variation of the angles α_{HWP} and (α_{QWP}) allows to extract the correlation values for different bases.

Visibility

The visibility can be used to parameterize the contrast of measured graphs. The visibility of a function $\tilde{f}(\theta)$ is defined as

$$\mathcal{V} = \frac{\max_\theta(\tilde{f}(\theta)) - \min_\theta(\tilde{f}(\theta))}{\max_\theta(\tilde{f}(\theta)) + \min_\theta(\tilde{f}(\theta))}, \tag{2.9}$$

where the optimisations (max and min) run over the angle θ. If one is now drawing a correlation function in dependence of an angle θ, this function can be bounded between -1 and 1. Thus, calculating the visibility of this function in the given way would lead to $\mathcal{V} = \frac{2}{0}$. To circumvent this problem when considering correlation functions, calculate a function $\tilde{f}^+(\theta)$ for the events of parity $+1$ and a function $\tilde{f}^-(\theta)$ for those of parity -1, i.e.

$$\tilde{f}^+(\theta) = f_{HH}(\theta) + f_{VV}(\theta) \tag{2.10}$$

$$\tilde{f}^-(\theta) = f_{HV}(\theta) + f_{VH}(\theta). \tag{2.11}$$

Now, we can calculate the visibilities of both functions such that $\mathcal{V}^+ = \frac{\max_\theta(\tilde{f}^+(\theta)) - \min_\theta(\tilde{f}^+(\theta))}{\max_\theta(\tilde{f}^+(\theta)) + \min_\theta(\tilde{f}^+(\theta))}$ indicates the visibility of the events of positive parity. $\mathcal{V}^-$ is found analogously.

From clicks to density matrix

We have seen in section 1.3 that a density matrix of a two qubit state can be written as follows:

$$\rho = \frac{1}{4} \sum_{i,j=0}^{3} s_{ij}\, \widehat{\sigma}_i \otimes \widehat{\sigma}_j \tag{2.12}$$

where the coefficients s_{ij} correspond to the K_{ij}^{ex}.

The sum contains 16 elements and consequently, 16 measurement values are needed to fully determine the density matrix of the state. The measurement of the whole set of

two-photon projectors based on the Pauli matrices $\{x, y, z\}$ requires 9 different settings. From these measurement 36 independent parameters can be extracted, i.e. the density matrix is over-determined.

The advantage of this method is that we can use the additional measurement results to obtain a better sensing of the state. For the calculation of the density matrix out of the experimental data Eqn. 2.12 can be expand:

$$\begin{aligned}\rho &= \frac{1}{4}\sum_{i,j=0}^{3} K_{ij}^{ex}\ \widehat{\sigma}_i \otimes \widehat{\sigma}_j = \\ &= \frac{1}{4}(K_{00}\ (1\otimes 1) + \sum_{i=1}^{3} K_{i0}^{ex}\ (\widehat{\sigma}_i \otimes 1) + \sum_{j=1}^{3} K_{0j}^{ex}\ (1 \otimes \widehat{\sigma}_j) + \sum_{i,j=1}^{3} K_{ij}^{ex}\ (\widehat{\sigma}_i \otimes \widehat{\sigma}_j))\end{aligned} \tag{2.13}$$

K_{00} is set to 1 due to the normalization and one gets three different kinds of correlations. K_{ij}^{ex} are the above mentioned correlations. K_{i0}^{ex} and K_{0j}^{ex} correspond to a local measurement, defined by tracing over the corresponding qubit. That's why each local correlation can be extracted by an average over three measurements [10]. For example, the K_{01}^{ex} corresponds to an average over three measurements of the basis settings XX, YX and ZX and they can be calculated:

$$\begin{aligned}K_{0j}^{ex} &= \frac{C_{HH} - C_{HV} + C_{VH} - C_{VV}}{C_{HH} + C_{HV} + C_{VH} + C_{VV}} \\ K_{i0}^{ex} &= \frac{C_{HH} + C_{HV} - C_{VH} - C_{VV}}{C_{HH} + C_{HV} + C_{VH} + C_{VV}}\end{aligned} \tag{2.14}$$

Example

Let us exemplarily consider the density matrix of the Bell state $|\psi^+\rangle = \frac{1}{\sqrt{2}}(|HV\rangle + |VH\rangle)$. The correlations of this state theoretical state $|\psi^+\rangle$ are found to be

For example, the theoretical correlation value of K_{XX} is 1, while $K_{X0} = 0$. According

	0	X	Y	Z
0	1	0	0	0
X	0	1	0	0
Y	0	0	1	0
Z	0	0	0	−1

to Eqn. 2.13, we can now assemble the density matrix ρ by using the correlation values and evaluating the tensor product of the respective Pauli matrices. Finally, we find for the density matrix

$$\rho = |\psi^+\rangle\langle\psi^+| = \begin{pmatrix} 0 & 0 & 0 & 0 \\ 0 & 0.5 & 0.5 & 0 \\ 0 & 0.5 & 0.5 & 0 \\ 0 & 0 & 0 & 0 \end{pmatrix}. \tag{2.15}$$

2.3 Software for the measurements

For the experiment two different programs are needed:

1. Count rates
2. Coincidence integration

Count rates

The detected coincidences can directly be watched in this program. Each detector is given the following position:

	mode A	mode B
H	2	8
V	1	4

The corresponding graphs show the single count rate of detectors (you can activate them simply by clicking on the corresponding symbol).
The coincidences count rates numbered as follows. For example,
$C_{HV} \mathrel{\widehat{=}}$ 'H(mode A) + V(mode B)' = 2+4=6

C_{HH}	C_{HV}	C_{VH}	C_{VV}
10	6	9	5

This program is very useful to adjust the relative phase ϕ with the YVO4 crystal and also to optimize the coupling into the two single mode fiber.

Coincidence integration

This program is started with a bash command. It is used for getting the measurement results. For this purpose it integrates the coincidence count rates over a certain time period which can be set in ms and writes them to a file.
Here the same logic as in the "Coincidence Count Rates" program is used, but the first item of the output-file is the overall count rate and therefore, one has to add +1 to the numbers shown above to find the coincidence count rates in the output files.

Linux commands

The software is run on a Linux machine. We suggest to use the program for reading out the coincidence counts and directly append the result into a file for each exercise. Assume the program is called with a command *X*, you can append the output of that command to a file ex1.dat by using "X >> ex1.dat". In case you directly want to see the result,

you can type “X >> ex1.dat && less ex1.dat”. This will open the programm *less*, which you can close by the shortcut “q”. If you want to delete a wrongly created file, type “rm ex1.dat”.

3 Experimentation

Please pay attention to the following points

- Never experiment without laser protection glasses. Already low intensities can harm your eyes permanently. The intensity of the laser beam is 100 times higher than the maximal limit for which a damage is probable.
- The used laser diode can be destroyed very easily by electrostatic charging. So please do not touch either the laser diode or the cables and avoid electrostatically charging yourself.
- Take care of the optical components. Please do not touch any surfaces of the lenses or the mirrors.
- Pay particular attention to the fiber optics. Do not touch them and do not put anything on them or on the two breadboards. Otherwise, the polarization of the photons can be shifted.
- Pay attention to the respective angle offsets of the waveplates. To compensate for the offset due to their mounting, all waveplates are labelled to indicate their 0° position. Add this given angle offset to the desired angle position.

Alignment

The alignment of the single components will be described in detail by the tutor.
An overview which components have to be adjusted before the measurement:

- The optomechanical components for coupling the laser beam to the single mode fiber optic
- YVO_4-crystal to align the phase

Experiments

1. **Measuring the correlation function**
   In this experiment two correlation function shall be detected. One HWP is set to 0° for the first measurement run and to 22.5° for the second. The other HWP is rotated in small steps to 90°. Why are measurements of correlation functions in two bases necessary to prove entanglement?

2. **Bell Inequality**
   In this setup a violate of the CHSH inequality can be obtained for the following measurement settings of the HWPs:

α	α'	β	β'
22.5°	0°	11.25°	-11.25°

3. **Quantum Tomography**

   The following table should help you to set the waveplates to the position needed for the respective measurement:

all in °		HWP A	HWP B	QWP A	QWP B
X	X	22.5	22.5	0	0
X	Y	22.5	0	0	45
X	Z	22.5	0	0	0
Y	X	0	22.5	45	0
Y	Y	0	0	45	45
Y	Z	0	0	45	0
Z	X	0	22.5	0	0
Z	Y	0	0	0	45
Z	Z	0	0	0	0

4. **Rotate the state to ψ^+**
   Put a HWP in one mode in front of the PA to rotate from H to V polarization. What angle α_{HWP} is need for this purpose?
   Measure the density matrix of this state.

5. **Rotate the state to ψ^-**
   Adjust the YVO4 crystal, so that a relative phase of π between HH and VV photon pairs is implemented.
   Measure the density matrix of this state.

6. **Rotate the state to ϕ^-**
   Measure the density matrix of this state.

Notation:

Schematic diagram of relative frequencies of the HH, HV, VH, VV coincidences facilitating the identification of the generated state:

	XX	YY	ZZ
ϕ^+	.5 0 0 .5	0 .5 .5 0	.5 0 0 .5
ψ^+	.5 0 0 .5	.5 0 0 .5	0 .5 .5 0
ψ^-	0 .5 .5 0	0 .5 .5 0	0 .5 .5 0
ϕ^-	0 .5 .5 0	.5 0 0 .5	.5 0 0 .5

Analysis

The following points should be described:

- generation of entangled photons
- experimental setup
- characteristical features of qubits and entanglement
- basics of quantum tomography.

With regard to the measurements, please

- discuss the measured correlation functions and answer the above question. Calculate for each of the two correlation function two visibility values as explained above,
- show the violation of the Bell inequality with a calculation of errors (assuming a Poissonian distribution of coincidences with the additional assumption that the total number of events is constant and hence without an error) and interpret your result, and
- calculate the density matrices of the produced states and discuss the results.

References

[1] Joseph B. Altepeter, Daniel F. V. James, and Paul G. Kwiat. 4 Qubit Quantum State Tomography. *Representations*, 145:113–145, 2004.

[2] Alain Aspect, Philippe Grangier, and Gérard Roger. Experimental Tests of Realistic Local Theories via Bell's Theorem. *Physical Review Letters*, 47:460–463, 1981.

[3] Achim Beetz. Die Bellschen Ungleichungen, 2005.

[4] John S. Bell. On the Einstein-Podolsky-Rosen paradox. *Physics*, 1:195–200, 1964.

[5] John F. Clauser, Michael A. Horne, Abner Shimony, and Richard A. Holt. Proposed Experiment to Test Local Hidden-Variable Theories. *Phys. Rev. Lett.*, 23(15):880–884, Oct 1969.

[6] Claude Cohen-Tannoudji, Bernard Diu, and Franck Laloe. *Quantum mechanics*. Quantum Mechanics. Wiley, 1977.

[7] Albert Einstein, Boris Podolsky, and Nathan Rosen. Can Quantum-Mechanical Description of Physical Reality Be Considered Complete? *Phys. Rev.*, 47(10):777–780, May 1935.

[8] Stuart J. Freedman and John F. Clauser. Experimental Test of Local Hidden-Variable Theories. *Phys. Rev. Lett.*, 28(14):938–941, Apr 1972.

[9] Daniel F. V. James, Paul G. Kwiat, William J. Munro, and Andrew G. White. Measurement of qubits. *Phys. Rev. A*, 64(5):052312, Oct 2001.

[10] Nikolai Kiesel. *Experiments on Multiphoton Entanglement*. PhD thesis, LMU München, 2007.

[11] Paul G. Kwiat, Edo Waks, Andrew G. White, Ian Appelbaum, and Philippe H. Eberhard. Ultrabright source of polarization-entangled photons. *Phys. Rev. A*, 60(2):R773–R776, Aug 1999.

[12] Leonard Mandel and Emil Wolf. *Optical Coherence and Quantum Optics*, volume 64. Cambridge University Press, 1995.

[13] Dieter Meschede. *Optik, Licht und Laser*. Teubner Studienbuecher. Teubner, 2005.

[14] Martin Schaeffer. Two-Photon Polarization Entanglement in Typ I SPDC Experiment. Bachelorthesis, LMU München, 2009.

[15] Thomas Scheidl, Rupert Ursin, Johannes Kofler, Sven Ramelow, Xiao-Song Ma, Thomas Herbst, Lothar Ratschbacher, Alessandro Fedrizzi, Nathan Langford, Thomas Jennewein, and Anton Zeilinger. Violation of local realism with freedom of choice. 2010.

[16] Christian I. T. Schmid. Kompakte Quelle verschränkter Photonen und Anwendungen in der Quantenkommunikation. Diplomarbeit, LMU München, 2004.

[17] Christian I. T. Schmid. *Multi-photon entanglement and applications in quantum information*. PhD thesis, LMU München, 2008.

[18] Erwin Schrödinger. Die gegenwärtige Situation in der Quantenmechanik. *Naturwissenschaften*, 23:807–812, 1935.

[19] Carsten Schuck. Experimental Implementation of a Quantum Game. Diplomarbeit, LMU München, 2003.

[20] M.O. Scully and M.S. Zubairy. *Quantum optics*. Cambridge University Press, 1997.

[21] Pavel Trojek. *Effcient Generation of Photonic Entanglement and Multiparty Quantum Communication*. PhD thesis, LMU München, 2007.

[22] Armin Uhlmann. The transition probability in the state space of a *-algebra. *Reports on Mathematical Physics*, 9:273–279, 1976.

[23] Jügen Volz. *Atom-Photon Entanglement*. PhD thesis, LMU München, 2006.

[24] Gregor Weihs, Thomas Jennewein, Christoph Simon, Harald Weinfurter, and Anton Zeilinger. Violation of Bell's Inequality under Strict Einstein Locality Conditions. *Phys. Rev. Lett.*, 81(23):5039–5043, Dec 1998.

[25] Witlef Wieczorek. *Multi-Photon Entanglement*. PhD thesis, LMU München, 2009.